Published in final edited form as:
Dev Dyn. 2003 November ; 228(3): 451–463.

Neurogenic Phenotype of *mind bomb* Mutants Leads to Severe Patterning Defects in the Zebrafish Hindbrain

Stephanie Bingham[1], **Summer Chaudhari**[1], **Gary Vanderlaan**[1], **Motoyuki Itoh**[2], **Ajay Chitnis**[2], and **Anand Chandrasekhar**[1,*]

[1]*Division of Biological Sciences, University of Missouri, Columbia, Missouri* [2]*Laboratory of Molecular Genetics, NICHD, NIH, Bethesda, Maryland*

Abstract

Failure of Notch signaling in zebrafish *mind bomb* (*mib*) mutants results in a neurogenic phenotype where an overproduction of early differentiating neurons is accompanied by the loss of later-differentiating cell types. We have characterized in detail the hindbrain phenotype of *mib* mutants. Hindbrain branchiomotor neurons (BMNs) are reduced in number but not missing in *mib* mutants. In addition, BMN clusters are frequently fused across the midline in mutants. Mosaic analysis indicates that the BMN patterning and fusion defects in the *mib* hindbrain arise non–cell autonomously. Ventral midline signaling is defective in the mutant hindbrain, in part due to the differentiation of some midline cells into neural cells. Interestingly, while early hindbrain patterning appears normal in *mib* mutants, subsequent rhombomere-specific gene expression is completely lost. The defects in ventral midline signaling and rhombomere patterning are accompanied by an apparent loss of neuroepithelial cells in the mutant hindbrain. These observations suggest that, by regulating the differentiation of neuroepithelial cells into neurons, Notch signaling preserves a population of non-neuronal cells that are essential for maintaining patterning mechanisms in the developing neural tube

Keywords

Zebrafish; hindbrain; motor neuron; induction; rhombomere; green fluorescent protein; neurogenesis; neuroepithelial cell; Notch–Delta signaling; ventral midline

INTRODUCTION

In the vertebrate neural tube, specific types of neurons and non-neuronal cells are generated from neuroepithelial cells in well-defined spatial and temporal patterns to permit normal growth, patterning, and function of the nervous system. The mechanisms that underlie the choice between specific neuronal and non-neuronal fates have been intensively studied in vertebrates and invertebrates. The highly conserved Notch–Delta signaling pathway has been demonstrated to play a central role in regulating production of different types of cells in both the nervous system and other tissues (Artavanis-Tsakonas et al., 1999). During vertebrate neural development, proneural gene expression defines domains in the neuroectoderm where cells have the potential to become neurons. Proneural genes drive expression of the Notch ligand, Delta. Delta activates Notch in neighboring cells and inhibits proneural gene function (and neuronal fate) in these cells in a process called lateral inhibition. In the absence of Notch-

*Correspondence to: Dr. Anand Chandrasekhar, Division of Biological Sciences, Room 205 Lefevre Hall, 0University of Missouri, Columbia, MO 65211. E-mail: anandc@missouri.edu.

mediated lateral inhibition, too many cells in the proneural domains differentiate into neurons, generating a neurogenic phenotype (Chitnis et al., 1995; de la Pompa et al., 1997).

Mutagenesis screens in zebrafish have identified several genetic loci that encode components of the Notch signaling pathway (Schier et al., 1996; Jiang et al., 1996). Mutations in *deltaD* (*after eight*) and *notch1* (*deadly seven*) result in weak neurogenic phenotypes (van Eeden et al., 1996; Holley et al., 2000, 2002; Gray et al., 2001), suggestive of partially redundant functions shared with other *notch* and *delta* genes. A dominant negative mutation in *deltaA* generates a strong neurogenic phenotype (Appel et al., 1999; Riley et al., 1999). Loss-of-function mutations in *mind bomb* (*mib*; Schier et al., 1996; Jiang et al., 1996), which encodes an E3 ubiquitin ligase required for effective Delta function (Itoh et al., 2003), result in a strong neurogenic phenotype (Schier et al., 1996; Jiang et al., 1996; van Eeden et al., 1996; Haddon et al., 1998b; Riley et al., 1999). In *mib* mutants, there is excess production of neurons born early in development (i.e., primary neurons), and a concomitant reduction in the number of later-born (secondary) neurons (Schier et al., 1996; Jiang et al., 1996; Itoh et al., 2003; Park and Appel, 2003). In a 24-hr mutant embryo, the developing spinal cord is nearly filled with cells expressing *huC* (Itoh et al., 2003; Park and Appel, 2003), an early neuronal differentiation marker (Kim et al., 1996; see also Lyons et al., 2003).

Analysis of zebrafish Notch signaling mutants, including *mib*, showed that this pathway regulates cell fate decisions in trunk midline tissues (Appel et al., 1999). Other studies of *mib* mutants have demonstrated the significance of Notch signaling in preventing precocious generation of primary neurons so that sufficient undifferentiated cells are retained to acquire alternate fates such as secondary neurons, glial cells, and neural crest-derived cell types (Jiang et al., 1996; Haddon et al., 1998b, Riley et al., 1999; Itoh et al., 2003; Park and Appel, 2003). However, little is known about other consequences of premature neuronal differentiation in *mib* mutants. For example, it is not clear whether excessive neurogenesis in *mib* mutants can lead to the loss of signaling tissues that regulate later development or interferes with processes that maintain segmental identity. In this report, we have examined the differentiation and organization of various hindbrain cell types such as branchiomotor neurons, interneurons, and ventral midline cells to understand the consequences of the *mib* neurogenic phenotype for hindbrain segmentation and ventral midline signaling. We found that severe defects in segmental patterning and midline signaling seen after 21 hr in the mutant hindbrain correlate with the premature and extensive formation of neuronal cells. We suggest that these deficits are due to the loss of neuroepithelial cells that are normally prevented from becoming neurons by Notch signaling, thus allowing them to serve essential roles in segmental patterning and midline signaling.

RESULTS

Premature Neuronal Differentiation in the *mind bomb* Mutant Hindbrain

To better understand the role of *mib* in hindbrain development, we monitored the expression of the panneuronal marker *huC* (Kim et al., 1996; see also Lyons et al., 2003) from early somitogenesis in embryos obtained from *mib* +/- crosses. In wild-type embryos, *huC*-expressing cells were restricted to the lateral margins of the hindbrain at all axial levels (Fig. 1A,C) at 17 hr postfertilization (hpf) and 24 hpf. In contrast, *mib* mutants contained large numbers of *huC*-expressing cells throughout the hindbrain (Fig. 1B,D). In addition, expression of a neurogenesis marker *deltaD* (Haddon et al., 1998a) was mostly absent in the mutant hindbrain at 24 hpf (Fig. 1E,F). These results indicate that a majority of cells at all axial levels in the mutant hindbrain initiate neuronal differentiation prematurely, with a concomitant loss of neuronal progenitor cells beyond 24 hpf.

To determine whether premature *huC* expression in the *mib* mutant hindbrain affected the development of later-born neurons, we examined the expression of a zebrafish *even-skipped* homolog *evx1*, which identifies *Dm-Grasp*-expressing (zn5/8 antibody-labeled) hindbrain commissural neurons and other interneurons (Trevarrow et al., 1990; Kanki et al., 1994; Fashena and Westerfield, 1999; Thaeron et al., 2000). In wild-type embryos, *evx1* was expressed in medial and lateral domains in the hindbrain from 24 hpf (Fig. 1G and data not shown; Thaeron et al., 2000). In *mib* mutants, *evx1*-expressing cells were reduced in number and disorganized (Fig. 1H). The loss of *evx1*-expressing commissural neurons between 24 and 36 hpf anticipates the observed loss of zn5/8 antibody-labeled commissural neurons in the mutant hindbrain at 36 hpf (Jiang et al., 1996). Thus, the premature widespread appearance of *huC*-expressing cells in the mutant hindbrain between 17 and 24 hpf correlates with the loss and disorganization of a hindbrain neuron type that begins to differentiate at 24 hpf.

Development of Hindbrain Motor Neurons Is Disrupted in *mind bomb* Mutants

Three major subtypes of hindbrain branchiomotor neurons (BMNs) in zebrafish are the nV, nVII, and nX neurons, which arise at different axial levels, with nV being the most rostral and nX the most caudal (Chandrasekhar et al., 1997; Higashijima et al., 2000; Chandrasekhar et al., 2003). Expression of the motor neuron marker *islet1* (Appel et al., 1995) appears first in nVII neurons at ~15 hpf, in nV neurons at ~18 hpf, and in nX neurons at ~24 hpf (Chandrasekhar et al., 1997; Higashijima et al., 2000). In wild-type embryos harboring the *islet1-GFP* transgene (Higashijima et al., 2000), the various BMN populations were found in normal numbers and locations, as previously described (Fig. 2A; Chandrasekhar et al., 1997; Higashijima et al., 2000). In *mib* mutants, the BMN clusters were smaller. Furthermore, the clusters were variably fused across the midline (Fig. 2B). Similarly, expression analysis of the zinc finger transcription factor *gata3* (Bingham et al., 2002) revealed that nV and nVII motor neurons were frequently reduced and fused across the midline in *mib* mutants, while other *gata3*-expressing hindbrain cells were absent (Fig. 2C,D). We quantified specific neuronal populations in the hindbrain and spinal cord by using an anti-islet monoclonal antibody (Korzh et al., 1993; Fig. 2E,F). As reported previously (Appel et al., 1999), the number of early differentiating Rohon–Beard neurons was substantially increased in the *mib* mutant spinal cord, with a concomitant decrease in the number of late-differentiating secondary motor neurons and interneurons (Table 1). In the *mib* hindbrain, the total number of BMNs spanning rhombomeres 2 through 7 was decreased by 46% compared with wild-type siblings (Fig. 2B,F; Table 1). Of interest, nV motor neurons, which begin to differentiate at 18 hpf, were less affected (27% loss) than nVII neurons (56% loss), which begin to differentiate at 15 hpf (Table 1). In addition, nX motor neurons, which begin to differentiate at 24 hpf in the caudal hindbrain were reduced but not absent in *mib* mutants (Fig. 2A,B). These data show that there is no correlation between the time of onset of differentiation and change in BMN numbers at all axial levels in the *mib* mutant hindbrain. However, the identities of other neurons generated from the same local precursor populations as specific BMN subtypes, and their fate in *mib* mutants, are not known (see Discussion section).

We tested whether the loss of BMNs in *mib* mutants reflects the loss of precursor cells that generate motor neurons in response to hedgehog signals by examining the effects of *shh* overexpression on BMN number in *mib* mutants (Fig. 3). *Shh* was overexpressed in *mib* mutants by injecting full-length *shh* RNA into embryos obtained from *mib* +/-; *islet1-GFP* +/- parents. In wild-type siblings, *shh* overexpression led to sharp increases in BMN number, especially in rhombomere 2 (r2) and r4 (Fig. 3A,C). Cell counts in islet antibody-labeled embryos revealed a 48% average increase over control wild-type siblings (Table 2), which is similar to previous results (Chandrasekhar et al., 1998). Importantly, *shh* overexpression also led to an increase in *GFP*-expressing cells in the *mib* mutant hindbrain (Fig. 3B,D), with a 42% average increase compared with control mutant embryos (Table 2). While many of the excess *GFP*-expressing

cells were located in the dorsal neural tube, as described previously (Chandrasekhar et al., 1998), many cells were also found in the ventral neural tube where the putative motor neuron precursor pools would be located (Fig. 3E–H). These data indicate that cells in the ventral neural tube of *mib* mutants can differentiate into the motor neurons in response to Shh, suggesting that precursor cells are still present in the mutant hindbrain. Furthermore, while the absolute number of BMNs is substantially lower in *mib* mutants, *shh* overexpression increases BMN number by roughly the same extent in wild-type (48%) and mutant (42%) embryos, suggesting that the motor neuron precursor pool is smaller in mutants.

While BMNs were frequently fused across the midline in *mib* mutants, the nV and nVII motor axons extended normally out of the hindbrain into the pharyngeal arches (Figs. 2B,3B). To test whether fusion of motor neuron clusters correlated with the absence of midline cues, we examined the development of the Mauthner reticulospinal neurons and their decussating axons in 36 hpf embryos by using the 3A10 antibody (Hatta, 1992). As demonstrated previously, the number of Mauthner neurons was greatly increased in *mib* mutants (Fig. 2B;Jiang et al., 1996). However, the Mauthner axons never aberrantly recrossed the midline in mutant embryos, even in regions with extensive fusion of putative nX motor neurons (Fig. 2B), indicating that midline cues (and ventral midline cells) required for Mauthner axon pathfinding (Hatta, 1992) were unaffected in the *mib* mutant hindbrain at the time when these early differentiating neurons extended axons.

Development of Ventral Tissues Is Defective in the *mind bomb* Mutant Hindbrain

Although Mauthner axon pathfinding is normal, the fusion of BMN clusters in *mib* mutants suggests that some aspects of midline tissue development may be affected in the mutant hindbrain. Indeed, specification of trunk midline cell fates is altered in *mib* mutants such that excess notochord cells are generated, with a concomitant loss of floor plate and hypochord cells (Appel et al., 1999). Therefore, we monitored floor plate development in the mutant hindbrain using *shh* expression as a marker (Krauss et al., 1993). Embryos were processed for *huC* and *shh* double in situ hybridizations to identify mutant embryos at younger ages (Fig. 4A–D). At 16.5 hpf and 21 hpf, *shh*-expressing floor plate cells were found throughout the hindbrain, without any gaps, in wild-type and mutant embryos (compare Fig. 4A,C with Fig. 4B,D). Although no obvious decrease in the number of floor plate cells was evident in *mib* mutants, it is possible that there is a small but significant reduction, similar to the spinal cord (Appel et al., 1999). In contrast, by 25 hpf, *shh* expression in *mib* mutants was displaced dorsally in some rhombomeres and missing in other regions, with a nonexpressing patch frequently coinciding with r4 (Fig. 4F; Table 3). Expression of another floor plate marker *axial* (Strahle et al., 1993) was similarly affected in 24 hpf *mib* mutants (data not shown). Expression of the Shh target gene *nk2.2* in the ventral neural tube (Barth and Wilson, 1995) was also patchy in the mutant hindbrain with a nonexpressing patch frequently coinciding with r4 (Fig. 4G,H; Table 3). Expression of the Shh-regulated axon guidance gene *net1b* in the ventral neural tube (Strahle et al., 1997) was maintained throughout the mutant hindbrain, but in a smaller number of cells than normal, with a distinctive gap frequently coinciding with r4 (Fig. 4I,J; Table 3). These results suggest that ventral tissues, including the midline, are significantly reduced, especially in r4, in *mib* mutant embryos.

If BMN fusion (Fig. 2B) were a consequence of defects in ventral midline signaling, it should be less evident before 21 hpf, when midline signaling appears normal in *mib* mutants. However, the nV and nVII neuron clusters were disorganized and variably fused in 18 hpf mutant embryos (Fig. 4K,L), indicating that these BMN defects arise before any obvious defects in *shh* expression at the ventral midline.

Relationship Between the *mind bomb* Ventral Midline and Neurogenic Phenotypes

Since gaps appear in the floor plate only after 21 hpf (Fig. 4F), we wondered whether the patchy loss of ventral midline tissue in *mib* mutants was linked to the extensive generation of *huC*-expressing cells in the mutant hindbrain (Fig. 1A–D). This issue was addressed by examining the arrangement of *huC*- and *shh*-expressing cells in the ventral hindbrain at different axial levels. Cross-sections of the hindbrain were prepared from wild-type and mutant embryos processed for *huC* or *huC; shh* in situ hybridizations. In 24 hpf wild-type hindbrains, *huC*-expressing cells were restricted to the lateral margins of the neural tube and excluded from the floor plate (Fig. 5A). In *mib* mutants, *huC*-expressing cells filled the hindbrain but were frequently excluded from the ventral midline, likely the floor plate cells (Fig. 5B). We confirmed this in two-color in situ hybridizations, which showed that the patch of non–*huC*-expressing cells at the ventral midline in mutants expressed *shh* (Fig. 5C,D). However, in mutant embryos, many ventral midline cells appeared to coexpress *shh* and *huC* (Fig. 5F). Furthermore, in hindbrain regions containing no *shh*-expressing cells, *huC*-expressing cells were often, but not always, located at the ventral midline, immediately dorsal to the notochord (Fig. 5E). These results suggest that the patchy loss of *shh* expression after 21 hpf in the *mib* hindbrain may result in part from the differentiation of *shh*-expressing floor plate cells into *huC*-expressing neural cells.

Defects in BMN Patterning in *mind bomb* Mutants Are Generated Non–Cell Autonomously

Previous studies have suggested that *mib* is required nonautonomously for effective Notch signaling (Itoh et al., 2003). Therefore, we tested whether the aberrant patterning and midline fusion phenotypes of BMNs of *mib* mutants also reflect a non–cell autonomous requirement for *mib* in the hindbrain.

Heterochronic transplants were performed using sphere stage donor embryos transgenic for *islet1-GFP* and labeled with rhodamine dextran and nontransgenic, unlabeled, shield stage host embryos (Fig. 6A). In control experiments, donor-derived wild-type cells that differentiated into *GFP*-expressing BMNs in wild-type host embryos formed clusters in the appropriate locations and did not fuse across the midline (Fig. 6B; 88 neurons, 2 embryos). In contrast, donor-derived wild-type motor neurons were positioned randomly within the *mib* mutant hindbrain. Wild-type cell bodies and axons frequently straddled the midline, reflecting the fusion phenotype, and indicating that the mutant environment dictates wild-type BMN patterning (Fig. 6C; 42 neurons, 3 embryos). Conversely, donor-derived *mib* mutant motor neurons were patterned normally in wild-type host hindbrains and never exhibited any midline fusion (Fig. 6D; 142 neurons, 4 embryos). These results demonstrate a nonautonomous requirement for *mib* in neural patterning, analogous to its previously defined role in Notch signaling (Itoh et al., 2003). The non-autonomous BMN patterning phenotype may result from defects in ventral midline signaling (Fig. 4) and rhombomere patterning (Fig. 7; see below) in *mib* mutants.

While performing the mosaic analysis, we noticed that wild-type cells transplanted into mutant embryos (Fig. 6C) seldom exhibited the columnar morphologies suggestive of neuroepithelial cells (compare with Fig. 6B,D). Therefore, we examined the morphologies of rhodamine-dextran labeled donor cells at higher magnification in 36 hpf wild-type and mutant hosts, and classified them as being neuroepithelial (columnar morphology) and neuronal (round cells with at least one short process; Fig. 6E,F; see Experimental Procedures section). Approximately 30% of labeled cells in each host background could not be scored for either morphology and were excluded from analysis. Approximately 98% of scored wild-type cells in *mib* mutants had neuronal morphology (Fig. 6F; 218/222 cells, 6 embryos). In sharp contrast, only 68% of scored donor cells (wild-type or mutant) in wild-type hosts exhibited neuronal morphology (Fig. 6E; 98/144 cells, 8 embryos), and approximately 30% of the cells exhibited

neuroepithelial morphologies. These observations suggest that the *mib* mutant environment is unable to either prevent transplanted wild-type cells from becoming neurons or preserve them as neuroepithelial cells.

Late, but not Early, Rhombomere Patterning Is Defective in *mind bomb* Mutants

Since neuroepithelial cells are essential for morphogenesis and patterning of the neural tube, including the hindbrain (Moens and Prince, 2002; Geldmacher-Voss et al., 2003), we monitored rhombomere patterning in *mib* mutants from 16.5 to 24 hpf, when the neurogenic phenotype becomes progressively severe (Fig. 7). Embryos from *mib* +/- crosses were processed for two-color in situ hybridizations with *huC* and *krox20* to monitor rhombomere organization in young embryos. *Krox20* (Oxtoby and Jowett, 1993) was expressed normally in rhombomeres 3 and 5 in 16.5 and 20 hpf *mib* mutants, even though excessive neurogenesis was evident in the mutant hindbrain (Fig. 7A–D). Furthermore, no defects in the expression of *hoxb1a* in r4 (Prince et al., 1998), and *valentino* in r5 and r6 (Moens et al., 1998) were observed in 18 hpf embryo clutches obtained from *mib* +/- crosses (data not shown). These data demonstrate that rhombomeres are formed and boundaries are established normally in mutant embryos. However, by 24 hpf, *krox20* expression in r3 and r5 (Fig. 7E) was severely reduced or absent in *mib* mutants (Fig. 7F). In addition, *hoxb1a* expression in r4 was greatly reduced in *mib* mutants, and the boundaries with adjacent compartments were poorly defined (Fig. 7E,F; see also Fig. 4E–H). We performed acridine orange staining on live embryos to monitor cell death patterns in the hindbrain (Brand et al., 1996). There were no differences in the distribution of dying cells between wild-type and mutant embryos at 24 and 36 hpf (data not shown), indicating that loss of rhombomere boundaries in mutants was not due to increased cell death. These results suggest strongly that the excessive differentiation of neurons between 16.5 and 24 hpf in *mib* mutants occurs at the expense of neuroepithelial cells that may be required for maintaining rhombomere identities and boundaries beyond 24 hpf.

DISCUSSION

Previous studies have shown that excess primary neurons are generated in *mib* mutants while secondary neurons are reduced (Jiang et al., 1996; Schier et al., 1996; Itoh et al., 2003; Park and Appel, 2003). In addition, neurogenesis genes such as *ngn1*, *zash1a*, *zash1b*, and *deltaD* are expressed ectopically and at high levels during early somitogenesis (10–18 hpf), but greatly reduced at subsequent stages (Jiang et al., 1996; Itoh et al., 2003). The production of neurons at a higher density within proneural domains at 12–13 hpf characterizes the initial neurogenic phenotype in *mib* mutants (Jiang et al., 1996; Itoh et al., 2003). However, between 17 and 24 hpf, the neurogenic phenotype becomes more expansive with most cells of the neural tube expressing the neuronal marker *huC* by 24 hpf (Fig. 1; Itoh et al., 2003; Park and Appel, 2003). These striking changes in the patterns of neurogenesis suggest that the failure of lateral inhibition in *mib* mutants permits too many neuronal precursors to differentiate early and assume the fate of early born neurons, depleting the neural tube of neuroepithelial cells that would otherwise have adopted alternate fates and contributed to the formation of later-born neurons. Our detailed analysis of cell differentiation and patterning in the hindbrain is consistent with this view. In addition, our studies suggest strongly that the extensive loss of neuroepithelial cells in *mib* mutants leads to severe secondary defects in patterning.

Potential Mechanisms Underlying BMN Loss in *mind bomb* Mutants

In the *mib* hindbrain, *huC*-expressing cells are sharply increased in number between 17 and 24 hpf, compared with wild-type, such that *evx1*-expressing neurons that normally appear at 24 hpf are reduced in mutants (Fig. 1). Therefore, we expected that early differentiating BMNs, such as the nVII neurons in rhombomere 4 (r4-r7), and the nV neurons in r2 and r3, which begin to differentiate at 15 hpf (nVII) and 18 hpf (nV), would be generated in excess in *mib*

mutants and that the nX BMNs, which begin to differentiate at 24 hpf in the caudal hindbrain, would be greatly reduced or missing. However, both the nV and nVII motor neurons are reduced in *mib* mutants, and significant numbers of nX neurons are induced (Fig. 2). There are several possible explanations. First, because nV and nVII neurons are born continuously over an extended time period beginning at 18 and 15 hpf, respectively, it is possible that nV and nVII neurons born early are indeed generated in excess in mutants, while the later-differentiating nV and nVII neurons are completely lost, leading to a variable net reduction in BMNs. Alternatively, although some BMN subtypes are born earlier than others, BMNs, as a whole, may represent a cell type that differentiates relatively late compared with other types of neurons generated from the same local precursor pools. Consequently, the reduction in BMNs in *mib* mutants may be the result of excessive formation of other earlier-born neurons, and the variable reduction in BMN subtypes may reflect the degree to which the early neurogenic phenotype depletes local precursor pools in different rhombomeres. However, in the absence of specific markers to distinguish between early- and late-born nV and nVII neurons or information about other neurons that might be generated earlier from the common precursor pools that generate BMNs, these models cannot be tested.

The *shh* overexpression experiments (Fig. 3) were originally performed to determine whether the loss of BMNs in *mib* mutants was due to a loss of precursor cells capable of responding to Shh or was due to a loss/reduction of Shh signal from the ventral midline. The results do not clearly distinguish between these possibilities. As shown previously in wild-type embryos (Chandrasekhar et al., 1998), *shh* overexpression induces ectopic BMNs in *mib* mutants in domains that include the ventral neural tube, indicating that Shh-responsive precursor pools are not completely depleted in mutants. In addition, while BMN number is increased by roughly similar extents (~45%) in wild-type and *mib* mutants after *shh* overexpression, the absolute number of neurons induced is lower in mutants (Table 2), consistent with the idea that Shh-responsive precursor pools are smaller in *mib* mutants. However, we cannot rule out that the patchy loss of *shh* expression at the ventral midline also contributes to the BMN deficit in *mib* mutants. Hence, although the precise mechanism that leads to the reduction in BMN number in *mib* mutants remains unclear, the observed deficits are likely to be, in part, secondary consequences of an early neurogenic phenotype.

Ventral Midline Defects in the *mind bomb* Mutant Hindbrain

Midline defects have been described previously in the trunk region of *mib* mutants (Appel et al., 1999), where there is a small (25%) but significant decrease in the number of floor plate and hypochord cells, and a corresponding increase in notochord cells. These and other data suggested that Notch–Delta signaling mediates cell fate decisions at the trunk midline (Appel et al., 1999). Because components of the Notch–Delta signaling pathway are expressed in the gastrula and tail bud organizer regions (Appel et al., 1999; Holley et al., 2002; Itoh et al., 2003), it is likely that Notch signaling also mediates midline cell fate decisions of the hindbrain region during gastrulation. There are two aspects to the ventral midline defects that we have described (Figs. 4, 5), one of which is consistent with a role for Notch signaling in determining floor plate fate in the ventral midline (Appel et al., 1999), whereas the other appears to be related to the role of the Notch pathway in regulating neurogenesis in the neural tube.

In the *mib* hindbrain, floor plate cells expressing *shh* are found in a continuous row (no gaps) between 15 and 21 hpf (Fig. 4B,D; data not shown). Furthermore, Mauthner axons, which extend through the hindbrain between 17 and 21 hpf (Mendelson, 1986; Hatta, 1992), pathfind normally in mutants (Fig. 2B), indicating that ventral midline cues necessary for Mauthner axon pathfinding (Hatta, 1992) are expressed normally in *mib* mutants. However, even though no obvious defect in floor plate development is evident in the 15–21 hpf mutant hindbrain, a small but significant reduction in the number of floor plate cells may have been missed. This

putative, early reduction in cell number could result directly from defective midline cell fate specification in the *mib* hindbrain during gastrulation (Appel et al., 1999). However, the second aspect of *mib* ventral midline defects is the appearance of gaps in *shh* and *axial* (and Shh-regulated *nk2.2* and *net1b*) expression after 21 hpf (Fig. 4E–J; data not shown). The gaps in *shh* expression can arise in at least two ways. First, an existing floor plate cell may down-regulate *shh* expression, perhaps due to trans-differentiation into another cell type. Alternatively, some daughter cells of mitoses in the floor plate may fail to differentiate into floor plate cells. Our results (Fig. 5) are consistent with both possibilities. In the *mib* hindbrain, while the domains of expression of the neural and floor plate markers (*huC* and *shh*, respectively) are mostly exclusive (Fig. 5A–D), there are numerous instances when the two genes appeared to be co-expressed at the ventral midline (Fig. 5F). In addition, wherever *shh*-expressing cells are missing (i.e., gaps in expression), *huC*-expressing cells are frequently found at the ventral midline, immediately dorsal to the notochord (Fig. 5E). Therefore, the patchy expression of *shh* at 24 hpf is likely not due to defective midline specification during gastrulation, but may result from the conversion of ventral midline cells into neuronal cells. This mechanism may also explain the consistent, but not absolute, loss (gap) of expression of *shh* and Shh-regulated target genes (*nk2.2*, *net1b*) in r4 in *mib* mutants (Fig. 4; Table 3). Premature and excessive neurogenesis, as evidenced by increased *zash1a* and *zash1b* expression, occurs first in r3/r4 at 16 hpf in mutants (Jiang et al., 1996), suggesting that the ventral midline cells in this hindbrain region may be especially susceptible to neuronal differentiation.

Genesis of Patterning Defects in *mind bomb* Mutants

In addition to a marked decrease in BMN number, the rhombomere-specific clustering of BMNs is lost in *mib* mutants. This defect may result directly from the dramatic loss of rhombomere-specific gene expression by 24 hpf. Of interest, rhombomere-specific gene expression in *mib* mutants is initiated correctly and maintained until approximately 21 hpf, by which time virtually the entire mutant hindbrain undergoes neuronal differentiation (Fig. 7). Rhombomere boundaries may be lost rapidly between 21 and 24 hpf due to the cumulative loss of cells that express molecules mediating repulsive cell–cell interactions (Xu et al., 1999;Cooke et al., 2001). In addition, the absence of zrf1-positive radial glial cells (Lyons et al., 2003), which are found at rhombomere boundaries (Trevarrow et al., 1990), in *mib* mutants (Jiang et al., 1996) may also play a role in the loss of rhombomere boundaries. Of interest, the radial glial cells in the zebrafish hindbrain are found in the ventricular zone, are mitotically active, and may give rise to neurons (Lyons et al., 2003), Therefore, the absence of these cells in *mib* mutants could have independent effects on rhombomere patterning and neurogenesis.

Although rhombomere boundaries and rhombomere-specific BMN organization are severely compromised in *mib* mutants, BMNs extend axons in a manner consistent with their anteroposterior location (Fig. 2B; data not shown). BMNs in the vicinity of r2 and r3 extend axons into the first branchial arch (nV neurons), whereas those in the vicinity of r4, r5, and r6 extend axons into the second branchial arch (nVII neurons). This observation suggests that the establishment and transient stability of rhombomere identity and boundaries up to ~21 hpf may be sufficient to impart region-specific identities to nV and nVII motor neurons. Our results are consistent with previous studies, which showed that failure to initiate and establish rhombomere-specific gene expression can lead to a complete loss of hindbrain compartment and BMN identities (Waskiewicz et al., 2002).

Role of Neuroepithelial Cell Loss in Generating the *mind bomb* Hindbrain Phenotype

The zebrafish neural tube forms by cavitation of the neural rod/keel, which is generated by an inward, convergent movement and a thickening of the neural plate, rather than by invagination, as in other vertebrates (Kimmel et al., 1995). Consequently, at the neural keel stage,

proliferation of neuroepithelial cells leads to bilaterally positioned daughter cells because their movement is not restricted by a central lumen (Kimmel et al., 1994; Geldmacher-Voss et al., 2003). Furthermore, the proliferative zone containing neuroepithelial cells is restricted to a well-defined layer immediately adjacent to the hindbrain ventricle (Lyons et al., 2003). Our observations suggest strongly that neuroepithelial cells are greatly reduced in number in *mib* mutants, especially after 21 hpf. First, quantification of cells with specific morphologies in wild-type and mutant hindbrains suggests that neuroepithelial cells are extremely rare in *mib* mutants at 36 hpf (Fig. 6), and this effect may be evident earlier. Second, while the ventricular zone of neuroepithelial cells is clearly defined in 24 hpf wild-type embryos, it is absent in *mib* mutants, because no ventricle is evident in cross-sections, and *huC*-expressing cells densely populate the entire neural tube in mutant embryos (Fig. 5). This phenotype is also obvious in cross-sections of *GFP*-expressing mutant embryos, where the various BMN subtypes, especially the nX neurons, are extensively clumped across the putative midline or ventricle (data not shown). Finally, at 16.5 hpf (neural keel stage), the rudiment of a central lumen, bordered by neuroepithelial cells, is visible in wild-type hindbrains and to a lesser degree in *mib* mutants (Fig. 7; data not shown). We propose that loss of neuroepithelial cells, especially after 21 hpf, leads to the patterning defects evident in *mib* mutants after 21 hpf. However, staining of live embryos with Bodipy ceramide to outline cell shapes (Cooper et al., 1999) has thus far not revealed any obvious differences in the number of neuroepithelial cells between wild-type and mutant hindbrains at 18 or 24 hpf (data not shown).

In conclusion, neural defects characterized in the *mib* mutant have thus far focused on the neurogenic phenotype of early born neurons, occurring at the cost of later-born neurons. Our data on BMN induction are consistent with this scenario. Moreover, the loss of BMN organization and rhombomere boundaries by 24 hpf in *mib* mutants underscores the importance of non-neuronal cells in maintaining patterning mechanisms. Our observations suggest strongly that premature neurogenesis in *mib* mutants leads to the extensive loss of neuroepithelial cells that have important roles in rhombomere boundary formation and midline signaling in the hindbrain. The potential roles of neuroepithelial cells in hindbrain patterning and ventral midline signaling processes can be studied in embryos where genetic or biochemical perturbation leads to severe disruption of neuroepithelial cell polarity and organization (Jiang et al., 1996; Pujic and Malicki, 2001; Geldmacher-Voss et al., 2003; Masai et al., 2003).

EXPERIMENTAL PROCEDURES

Animals

Zebrafish were reared and maintained as described in Westerfield (1995). Embryos were collected from pairwise matings, and developed at 28.5°C in E3 embryo medium (Bingham et al., 2002). Throughout the text, the developmental age of the embryos corresponds to the hours elapsed since fertilization (hours postfertilization, hpf). Embryos were transferred to E3 medium containing phenylthiourea between 18 and 22 hpf to prevent pigmentation. The *mind bomb* mutants (mib^{ta52b}) were identified on the basis of the morphology of the tectum and hindbrain at 24 hpf (Jiang et al., 1996). For analysis of branchiomotor neuron development, the motor neuron-expressed *GFP* transgene (Higashijima et al., 2000) was crossed into the *mib* mutant background.

Immunohistochemistry and In Situ Hybridization

Whole-mount immunohistochemistry was performed with various antibodies as described previously (Chandrasekhar et al., 1997; Bingham et al., 2002). Synthesis of digoxigenin-and fluorescein-labeled probes, whole-mount in situ hybridization, and two-color development were carried out as described previously (Chandrasekhar et al., 1997; Prince et al., 1998; Bingham et al., 2002). Embryos were deyolked, mounted in glycerol, and examined with an

Olympus BX60 microscope. In all comparisons, at least 10 wild-type and 10 mutant embryos were examined. For sectioning, embryos were gently deyolked in glycerol, transferred to PBS (Westerfield, 1995) and embedded in 7% agarose (Ultra Low Melting Point Agarose, Fisher). Sections (50 μm) were made by using a Vibratome 1000 Plus system and were mounted in glycerol.

Confocal Microscopy

Confocal imaging was carried out on live or fixed embryos embedded in a dorsal orientation in 1.2% agarose. Images were captured on an Olympus IX70 microscope equipped with a Bio-Rad Radiance 2000 confocal laser system. For obtaining virtual cross-sections, the *GFP*-expressing cell bodies at a given axial level were identified and boxed. Metamorph software rotated the Z-stacks within the boxed area 90 degrees to provide a cross-sectional view.

For quantifying cellular morphologies, 30–40 Z-sections (×40 magnification) of 2 μm thickness were obtained at the level of the otic vesicle in the ventral neural tube, where the rhodamine–dextran labeled donor-derived cells were located. Four consecutive sections were stacked, and the resulting nonoverlapping Z-stacks were scored for cellular morphologies, taking care not to count the same cell twice. Cells were classified as neuroepithelial if they exhibited columnar morphology (Fig. 6E) and as neuronal if they were round and possessed at least one dendritic process (Fig. 6F).

RNA Injections

Synthesis of full-length *shh* RNA was carried out as described previously (Chandrasekhar et al., 1998). RNA (~1 ng/embryo) was injected into one- to eight-cell stage embryos as described previously (Chandrasekhar et al., 1998).

Quantification of Neuronal Populations

Islet antibody-labeled nuclei of hindbrain neurons, ventral spinal cord neurons, and Rohon–Beard cells were counted in strongly labeled, preparations of 36 hpf embryos. Counts were performed under ×40 magnification.

Mosaic Analysis

Gastrula stage transplants and analysis of motor neuron development were performed essentially as described previously (Moens and Fritz, 1999; Jessen et al., 2002).

Acknowledgements

We thank the reviewers for valuable comments, Christine Thisse and Bernard Thisse for the *evx1* probe, Hitoshi Okamoto for the *islet1-GFP* fish, and Keqing Zhang, Moe Baccam, and Amy Foerstel for excellent fish care. We also thank Cathy Krull and Sinead O'Connell for equipment and help with Vibratome sectioning. This work was supported by a NSF-MAGEP fellowship (S.B.), undergraduate research internships from the University of Missouri LS-UROP program (S.C.), and the NIH (A.C.).

Grant sponsor: National Institutes of Health; Grant number: NS40449.

References

Appel B, Korzh V, Glasgow E, Thor S, Edlund T, Dawid IB, Eisen JS. Motoneuron fate specification revealed by patterned LIM homeobox gene expression in embryonic zebrafish. Development 1995;121:4117–4125. [PubMed: 8575312]

Appel B, Fritz A, Westerfield M, Grunwald DJ, Eisen JS, Riley BB. Delta-mediated specification of midline cell fates in zebrafish embryos. Curr Biol 1999;9:247–256. [PubMed: 10074451]

Artavanis-Tsakonas S, Rand MD, Lake RJ. Notch signaling: cell fate control and signal integration in development. Science 1999;284:770–776. [PubMed: 10221902]

Barth KA, Wilson SW. Expression of zebrafish *nk22* is influenced by *sonic hedgehog/vertebrate hedgehog-1* and demarcates a zone of neuronal differentiation in the embryonic forebrain. Development 1995;121:1755–1768. [PubMed: 7600991]

Bingham S, Higashijima S, Okamoto H, Chandrasekhar A. The zebrafish trilobite gene is essential for tangential migration of branchiomotor neurons. Dev Biol 2002;242:149–160. [PubMed: 11820812]

Brand M, Heisenberg CP, Jiang YJ, Beuchle D, Lun K, Furutani-Seiki M, Granato M, Haffter P, Hammerschmidt M, Kane DA, Kelsh RN, Mullins MC, Odenthal J, van Eeden FJ, Nusslein-Volhard C. Mutations in zebrafish genes affecting the formation of the boundary between midbrain and hindbrain. Development 1996;123:179–190. [PubMed: 9007239]

Chandrasekhar A, Moens CB, Warren JT Jr, Kimmel CB, Kuwada JY. Development of branchiomotor neurons in zebrafish. Development 1997;124:2633–2644. [PubMed: 9217005]

Chandrasekhar A, Warren JT Jr, Takahashi K, Schauerte HE, van Eeden FJM, Haffter P, Kuwada JY. Role of sonic hedgehog in branchiomotor neuron induction in zebrafish. Mech Dev 1998;76:101–115. [PubMed: 9767138]

Chandrasekhar A. Turning heads: development of vertebrate branchiomotor neurons. Dev Dyn. 2003in press

Chitnis A, Henrique D, Lewis J, Ish-Horowicz D, Kintner C. Primary neurogenesis in Xenopus embryos regulated by a homologue of the Drosophila neurogenic gene Delta. Nature 1995;375:761–766. [PubMed: 7596407]

Cooke J, Moens C, Roth L, Durbin L, Shiomi K, Brennan C, Kimmel C, Wilson S, Holder N. Eph signalling functions downstream of Val to regulate cell sorting and boundary formation in thecaudalhindbrain. Development 2001;128:571–580. [PubMed: 11171340]

Cooper MS, D'Amico LA, Henry CA. Confocal microscopic analysis of morphogenetic movements. Methods Cell Biol 1999;59:179–204. [PubMed: 9891361]

de la Pompa JL, Wakeham A, Correia KM, Samper E, Brown S, Aguilera RJ, Nakano T, Honjo T, Mak TW, Rossant J, Conlon RA. Conservation of the Notch signalling pathway in mammalian neurogenesis. Development 1997;124:1139–1148. [PubMed: 9102301]

Fashena D, Westerfield M. Secondary motoneuron axons localize DM-GRASP on their fasciculated segments. J Comp Neurol 1999;406:415–424. [PubMed: 10102505]

Geldmacher-Voss B, Reugels AM, Pauls S, Campos-Ortega JA. A 90 degrees rotation of the mitotic spindle changes the orientation of mitoses of zebrafish neuroepithelial cells. Development 2003;130:3767–3780. [PubMed: 12835393]

Gray M, Moens CB, Amacher SL, Eisen JS, Beattie CE. Zebrafish deadly seven functions in neurogenesis. Dev Biol 2001;237:306–323. [PubMed: 11543616]

Haddon C, Smithers L, Schneider-Maunoury S, Coche T, Henrique D, Lewis J. Multiple delta genes and lateral inhibition in zebrafish primary neurogenesis. Development 1998a;125:359–370. [PubMed: 9425132]

Haddon C, Jiang YJ, Smithers L, Lewis J. Delta-Notch signalling and the patterning of sensory cell differentiation in the zebrafish ear: evidence from the mind bomb mutant. Development 1998b; 125:4637–4644. [PubMed: 9806913]

Hatta K. Role of the floor plate in axonal patterning in the zebrafish CNS. Neuron 1992;9:629–642. [PubMed: 1382472]

Higashijima S, Hotta Y, Okamoto H. Visualization of cranial motor neurons in live transgenic zebrafish expressing green fluorescent protein under the control of the islet-1 promoter/enhancer. J Neurosci 2000;20:206–218. [PubMed: 10627598]

Holley SA, Geisler R, Nusslein-Volhard C. Control of her1 expression during zebrafish somitogenesis by a delta-dependent oscillator and an independent wave-front activity. Genes Dev 2000;14:1678–1690. [PubMed: 10887161]

Holley SA, Julich D, Rauch GJ, Geisler R, Nusslein-Volhard C. her1 and the notch pathway function within the oscillator mechanism that regulates zebrafish somitogenesis. Development 2002;129:1175–1183. [PubMed: 11874913]

Itoh M, Kim CH, Palardy G, Oda T, Jiang YJ, Maust D, Yeo SY, Lorick K, Wright GJ, Ariza-McNaughton L, Weissman AM, Lewis J, Chandrasekharappa SC, Chitnis AB. Mind bomb is a ubiquitin ligase

that is essential for efficient activation of Notch signaling by Delta. Dev Cell 2003;4:67–82. [PubMed: 12530964]

Jessen JR, Topczewski J, Bingham S, Sepich DS, Marlow F, Chandrasekhar A, Solnica-Krezel L. Zebrafish trilobite identifies new roles for Strabismus in gastrulation and neuronal movements. Nat Cell Biol 2002;8:610–615. [PubMed: 12105418]

Jiang YJ, Brand M, Heisenberg CP, Beuchle D, Furutani-Seiki M, Kelsh RN, Warga RM, Granato M, Haffter P, Hammerschmidt M, Kane DA, Mullins MC, Odenthal J, van Eeden FJ, Nusslein-Volhard C. Mutations affecting neurogenesis and brain morphology in the zebrafish,*Daniorerio*. Development 1996;123:205–216. [PubMed: 9007241]

Kanki JP, Chang S, Kuwada JY. The molecular cloning and characterization of potential chick *DM-GRASP* homologs in zebrafish and mouse. J Neurobiol 1994;25:831–845. [PubMed: 8089660]

Kim CH, Ueshima E, Muraoka O, Tanaka H, Yeo SY, Huh TL, Miki N. Zebrafish *elav*/HuC homologue as a very early neuronal marker. Neurosci Lett 1996;216:109–112. [PubMed: 8904795]

Kimmel CB, Warga RM, Kane DA. Cell cycles and clonal strings during formation of the zebrafish central nervous system. Development 1994;120:265–276. [PubMed: 8149908]

Kimmel CB, Ballard WW, Kimmel SR, Ullmann B, Schilling TF. Stages of embryonic development of the zebrafish. Dev Dyn 1995;203:253–310. [PubMed: 8589427]

Korzh V, Edlund T, Thor S. Zebrafish primary neurons initiate expression of the LIM homeodomain protein Isl-1 at the end of gastrulation. Development 1993;118:417–425. [PubMed: 8223269]

Krauss S, Concordet JP, Ingham PW. A functionally conserved homolog of the *Drosophila* segment polarity gene *hh* is expressed in tissues with polarizing activity in zebrafish embryos. Cell 1993;75:1431–1444. [PubMed: 8269519]

Lyons DA, Guy AT, Clarke JD. Monitoring neural progenitor fate through multiple rounds of division in an intact vertebrate brain. Development 2003;130:3427–3436. [PubMed: 12810590]

Masai I, Lele Z, Yamaguchi M, Komori A, Nakata A, Nishiwaki Y, Wada H, Tanaka H, Nojima Y, Hammerschmidt M, Wilson SW, Okamoto H. N-cadherin mediates retinal lamination, maintenance of forebrain compartments and patterning of retinal neurites. Development 2003;130:2479–2494. [PubMed: 12702661]

Mendelson B. Development of reticulospinal neurons of the zebrafish II Early axonal outgrowth and cell body position. J Comp Neurol 1986;251:172–184. [PubMed: 3782497]

Moens CB, Fritz A. Techniques in neural development. Methods Cell Biol 1999;59:253–272. [PubMed: 9891364]

Moens CB, Prince VE. Constructing the hindbrain: insights from the zebrafish. Dev Dyn 2002;224:1–17. [PubMed: 11984869]

Moens CB, Cordes SP, Giorgianni MW, Barsh GS, Kimmel CB. Equivalence in the genetic control of hindbrain segmentation in fish and mouse. Development 1998;125:381–391. [PubMed: 9425134]

Oxtoby E, Jowett T. Cloning of the zebrafish *krox-20* gene (*krx-20*) and its expression during hindbrain development. Nucleic Acids Res 1993;21:1087–1095. [PubMed: 8464695]

Park HC, Appel B. Delta-Notch signaling regulates oligodendrocyte specification. Development 2003;130:3747–3755. [PubMed: 12835391]

Prince VE, Moens CB, Kimmel CB, Ho RK. Zebrafish hox genes: expression in the hindbrain region of wild-type and mutants of the segmentation gene, valentino. Development 1998;125:393–406. [PubMed: 9425135]

Pujic Z, Malicki J. Mutation of the zebrafish glass onion locus causes early cell-nonautonomous loss of neuroepithelial integrity followed by severe neuronal patterning defects in the retina. Dev Biol 2001;234:454–469. [PubMed: 11397013]

Riley BB, Chiang M, Farmer L, Heck R. The deltaA gene of zebrafish mediates lateral inhibition of hair cells in the inner ear and is regulated by pax21. Development 1999;126:5669–5678. [PubMed: 10572043]

Schier AF, Neuhauss SC, Harvey M, Malicki J, Solnica KL, Stainier DY, Zwartkruis F, Abdelilah S, Stemple DL, Rangini Z, Yang H, Driever W. Mutations affecting the development of the embryonic zebrafish brain. Development 1996;123:165–178. [PubMed: 9007238]

Strahle U, Blader P, Henrique D, Ingham PW. Axial, a zebrafish gene expressed along the developing body axis, shows altered expression in cyclops mutant embryos. Genes Dev 1993;7:1436–1446. [PubMed: 7687227]

Strahle U, Fischer N, Blader P. Expression and regulation of a *netrin* homologue in the zebrafish embryo. Mech Dev 1997;62:147–160. [PubMed: 9152007]

Thaeron C, Avaron F, Casane D, Borday V, Thisse B, Thisse C, Boulekbache H, Laurenti P. Zebrafish evx1 is dynamically expressed during embryogenesis in subsets of interneurones, posterior gut and urogenital system. Mech Dev 2000;99:167–172. [PubMed: 11091087]

Trevarrow B, Marks DL, Kimmel CB. Organization of hindbrain segments in the zebrafish embryo. Neuron 1990;4:669–679. [PubMed: 2344406]

van Eeden FJ, Granato M, Schach U, Brand M, Furutani-Seiki M, Haffter P, Hammerschmidt M, Heisenberg CP, Jiang YJ, Kane DA, Kelsh RN, Mullins MC, Odenthal J, Warga RM, Allende ML, Weinberg ES, Nusslein-Volhard C. Mutations affecting somite formation and patterning in the zebrafish, *Danio rerio*. Development 1996;123:153–164. [PubMed: 9007237]

Waskiewicz AJ, Rikhof HA, Moens CB. Eliminating zebrafish pbx proteins reveals a hindbrain ground state. Dev Cell 2002;3:723–733. [PubMed: 12431378]

Westerfield, M. The zebrafish book. Eugene, OR: University of Oregon; 1995.

Xu Q, Mellitzer G, Robinson V, Wilkinson DG. In vivo cell sorting in complementary segmental domains mediated by Eph receptors and ephrins. Nature 1999;399:267–271. [PubMed: 10353250]

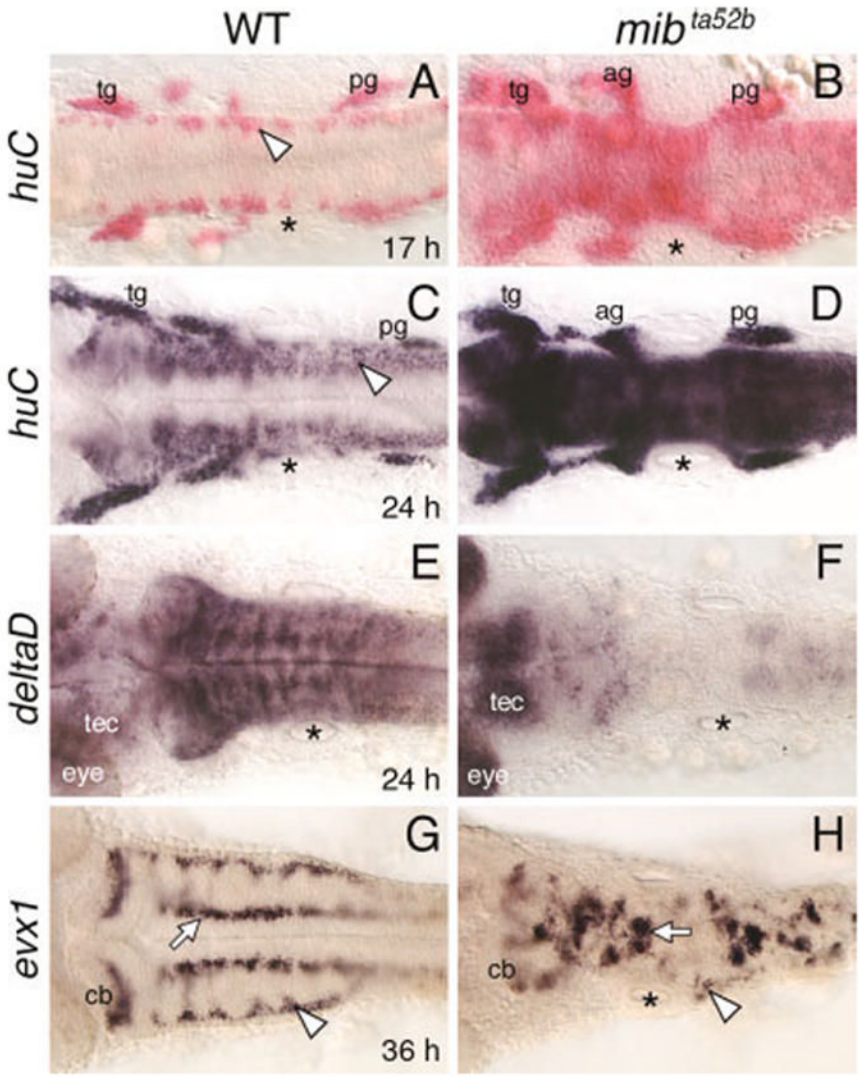

Fig. 1.

Defective neurogenesis in the *mind bomb* mutant hindbrain. All panels show dorsal views of the hindbrain with anterior to the left. The asterisks in all panels indicate the location of the otocyst. **A,B:** In a 17 hours postfertilization (hpf) wild-type embryo (WT; A), *huC* is expressed in small clusters of cells (arrowhead) located at the lateral margins of the hindbrain. In a *mib* mutant (B), *huC*-expressing cells are found throughout the hindbrain, with higher densities at some axial levels. **C,D:** In a 24 hpf wild-type embryo (C), the *huC* expression domain has expanded medially, and expressing cells are found at all axial levels, including the caudal hindbrain (arrowhead). In a *mib* mutant (D), the hindbrain at all axial levels is filled with *huC*-expressing cells. **E,F:** In a 24 hpf wild-type embryo (E), *deltaD* is expressed extensively, with higher expression in segmentally reiterated cell clusters. In the *mib* mutant (F), *deltaD* expression is greatly reduced or absent in the hindbrain and sharply higher in the tectum (tec) and eye. **G,H:** In a 36 hpf wild-type embryo (G), *evx1* is expressed in commissural neurons (arrowhead), cerebellar neurons (cb), and putative interneurons (arrow). In a *mib* mutant (H), the *evx1*-expressing commissural neurons are greatly reduced (arrowhead), while the cerebellar neurons and interneurons (arrow) are disorganized and fused, and reduced in number. ag, acoustic ganglion; cb, cerebellum; tec, tectum; tg, trigeminal ganglion; pg, posterior lateral line ganglion.

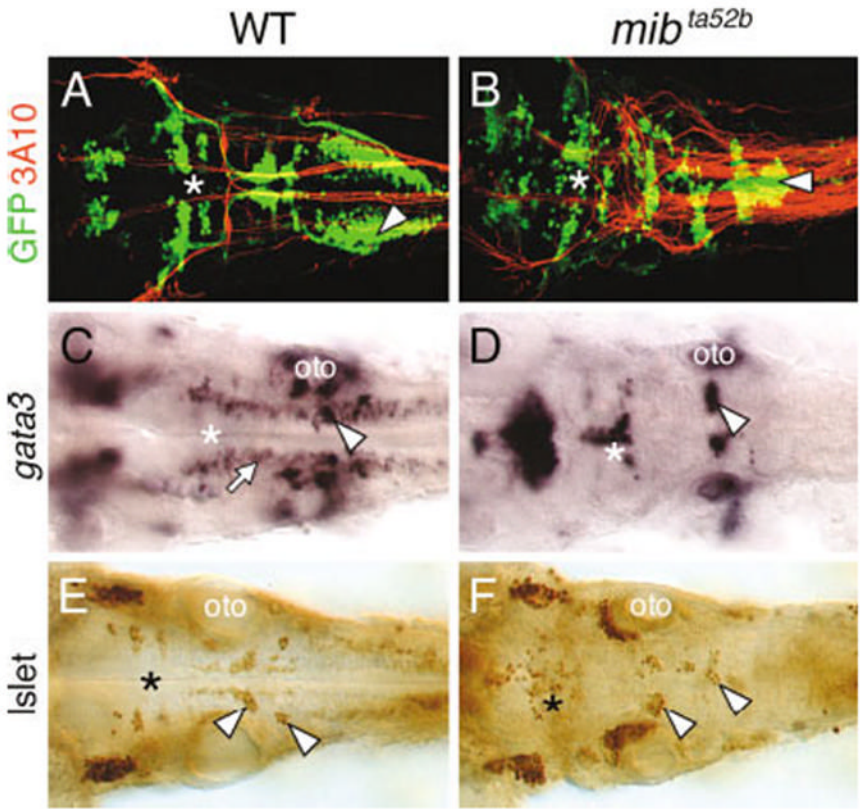

Fig. 2.

Branchiomotor neuron (BMN) development is severely disrupted in the *mind bomb* mutant hindbrain. All panels show dorsal views of the hindbrain with anterior to the left. A and B are composite confocal images and identify *GFP*-expressing motor neurons in the fluorescein channel and 3A10-labeled Mauthner (M) reticulospinal neurons and axons in the rhodamine channel. The asterisks in all panels indicate the location of the trigeminal motor neurons in rhombomeres 2 and 3. **A,B:** In a 36 hpf wild-type embryo (WT; A), the BMN clusters are found in their characteristic locations and numbers. The 3A10 antibody-labeled Mauthner cell axons decussate and descend contralaterally into the spinal cord. In a *mib* mutant (B), The BMNs clusters are disorganized and are variably fused. The supernumerary M cell axons cross the midline and descend contralaterally in a normal manner, whereas the nX motor neurons (arrowhead) in the same region exhibit extensive fusion across the midline. **C,D:** In a 36 hpf wild-type embryo (C), *gata3* is expressed by putative interneurons (arrow) and the nVII (arrowhead) and nV motor neurons (asterisk). In a *mib* mutant (D), *gata3*-expressing motor neurons (arrowhead, asterisk) are disorganized and the putative interneurons are absent. **E,F:** In a 36 hpf *mib* mutant (F), islet antibody-labeled BMNs (asterisk, arrowheads) are disorganized and variably fused and are reduced in number compared with wild-type siblings (E). oto, otocyst.

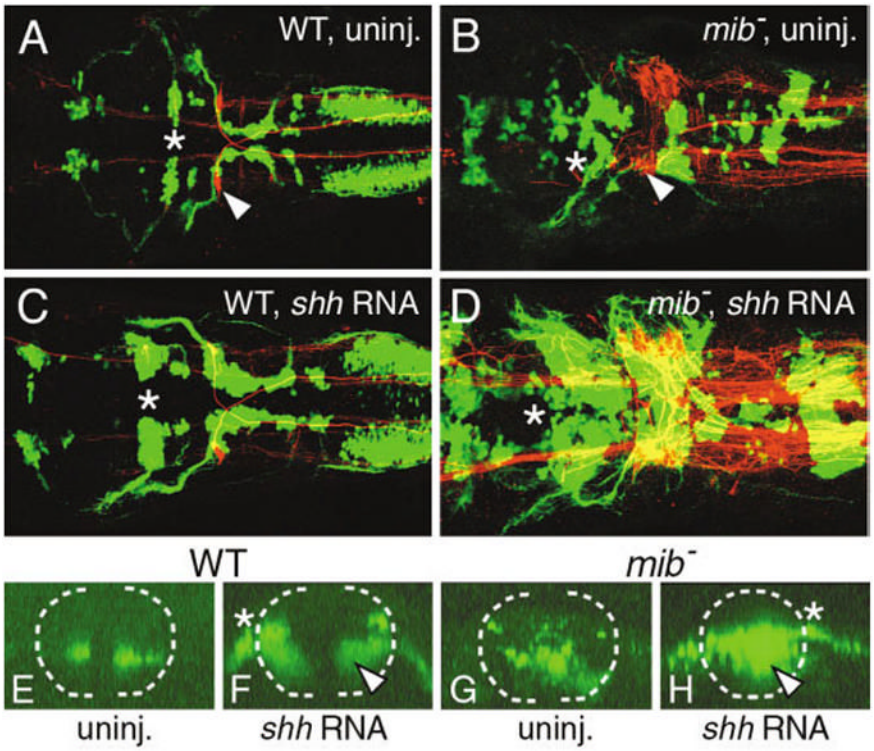

Fig. 3.

Shh overexpression induces branchiomotor neurons (BMNs) in the *mind bomb* mutant hindbrain. A–D show dorsal views of the hindbrain with anterior to the left and are composite confocal images, identifying *GFP*-expressing motor neurons in the fluorescein channel and 3A10-labeled Mauthner reticulospinal neurons and axons in the rhodamine channel. Asterisks in A–D indicate the location of the trigeminal (nV) motor neurons in rhombomere 2 (r2). E–H show confocal projections (virtual cross-sections) of *GFP*-expressing cells at the level of r4 and r5, and illustrate the effects of *shh* overexpression on nVII motor neurons. The broken line marks the outline of the neural tube, with dorsal to the top. The asterisks in F and H indicate the exit point of nVII axons from the neural tube. **A:** In a control wild-type embryo (WT), one Mauthner (M) neuron (arrowhead) is found on each side in r4 and BMNs are found in characteristic locations and numbers. **E:** In addition, the nVII motor neuron cell bodies are found in the ventral neural tube. **C:** In a *shh* RNA-injected wild-type embryo, the various *GFP*-expressing BMN clusters contain significantly larger numbers of cells, while M cell number is not affected. **F:** While most of the ectopic nVII motor neurons are found in the dorsal neural tube, a significant number (arrowhead) is also found in ventral locations. **B:** In a control *mib* mutant, there are excess M cells (arrowhead) and the BMNs exhibit the *mib* mutant phenotype. **G:** The nVII neurons are distributed randomly in the ventral half of the neural tube. **D:** Upon *shh* RNA injection, there is a sharp increase in the various BMN populations, while M cell number is not affected. **H:** Significantly, many of the ectopic nVII motor neurons (arrowhead) in the mutant are found in the ventral neural tube. The mutant embryo shown in D had an unusually large increase in motor neuron number at all axial levels.

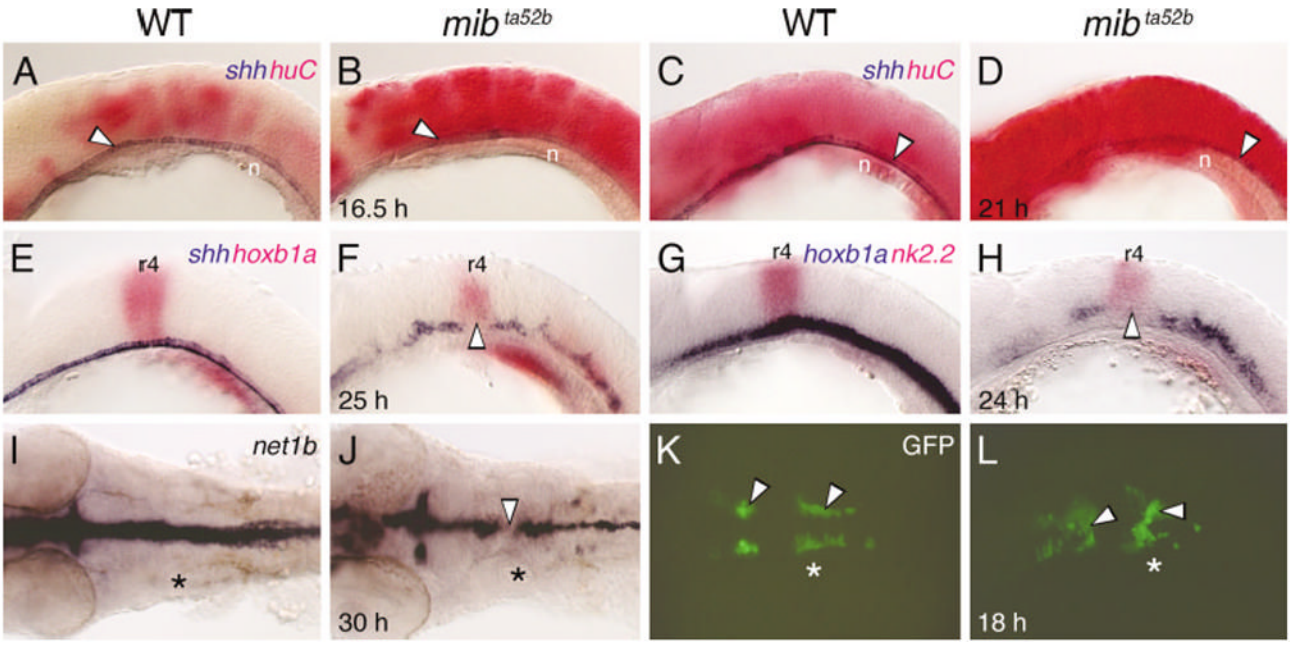

Fig. 4.

Development of ventral neural tube tissue is defective in the *mind bomb* hindbrain. A–H show lateral views and I–L show dorsal views of the hindbrain, with anterior to the left. Asterisks (I–L) indicate the location of the otocyst. **A–D:** At 16.5 hours postfertilization (hpf; A,B) and 21 hpf (C,D), *shh*-expressing floor plate cells (arrowheads) are found in a continuous row in wild-type (WT) and *mib* mutant embryos, even though *huC*-expressing cells are greatly increased in the mutant (B, D). **E,F:** In a 24 hpf *mib* mutant (F), *shh*-expressing floor plate cells are disorganized and slightly reduced in number compared with a wild-type sibling (E), with an absence of expressing cells in rhombomere 4 (r4, arrowhead), which is identified by *hoxb1a* expression. **G,H:** In a 24 hpf *mib* mutant (H), expression of *nk2.2* in the ventral neural tube is greatly reduced compared with a wild-type embryo (G), with an absence of expression in r4 (arrowhead). **I,J:** In a 30 hpf *mib* mutant (J), *net1b* expression is reduced at all axial levels compared with wild-type (I), with a gap of nonexpression in r4 (arrowhead). **K,L:** In an 18 hpf wild-type embryo (K), *GFP*-expressing nV and nVII motor neurons (arrowheads) are found bilaterally in r2 (nV neurons) and in a longitudinal column spanning r4 and r5 (nVII neurons). In a *mib* mutant (L), the motor neuron clusters (arrowheads) are disorganized, with considerable fusion across the midline. n, notochord.

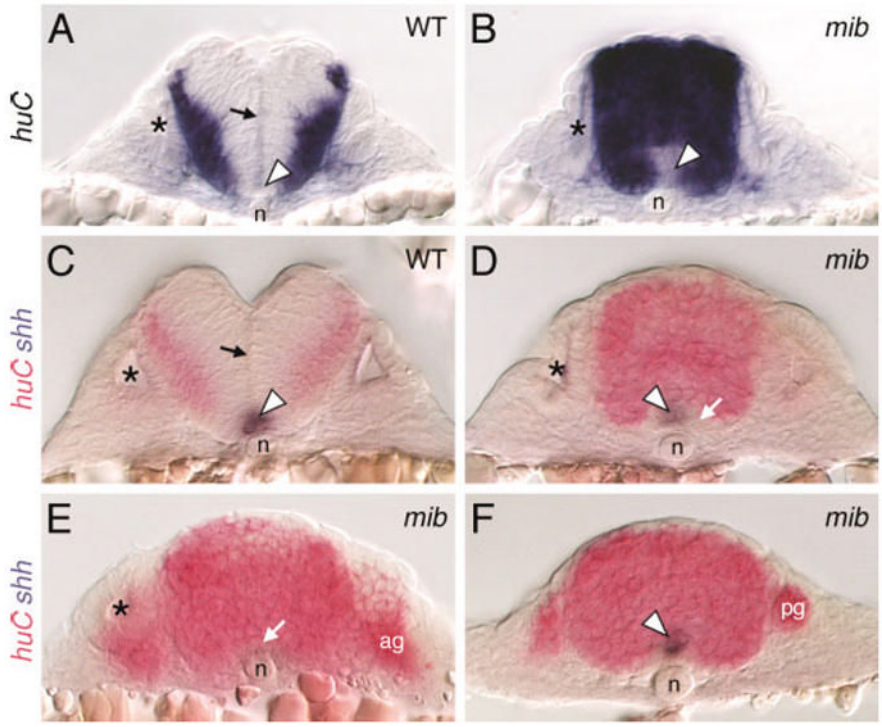

Fig. 5.

Distribution of neural cells in the *mind bomb* mutant hindbrain. All panels show cross-sections of the hindbrain in 24 hours postfertilization embryos at the level of rhombomere 5 (A–D), rhombomere 4 (E), and the caudal hindbrain (F). Asterisks in A–E identify the otocyst. **A,C:** In wild-type (WT) embryos, the *huC*-expressing cells are found at the lateral margins of the neural tube, outside the ventricular zone along the middle of the neural tube (arrows). The ventral midline contains floor plate cells (arrowheads) that express *shh* (C). **B,D:** In *mib* mutants, the entire neural tube is filled with *huC*-expressing cells, except at the ventral midline (arrowhead in B), which contains *shh*-expressing cells (arrowhead in D) and other cells that express neither *shh* nor *huC* (arrow in D). The ventricular zone is absent in mutant embryos. **E:** In this mutant, *huC*-expressing cells (arrow) occupy the ventral midline immediately dorsal to the notochord, and no *shh*-expressing cells are found. **F:** In this mutant, the ventral midline cells coexpress *shh* and *huC* (arrowhead). ag, acoustic ganglion; n, notochord; pg, posterior lateral line ganglion.

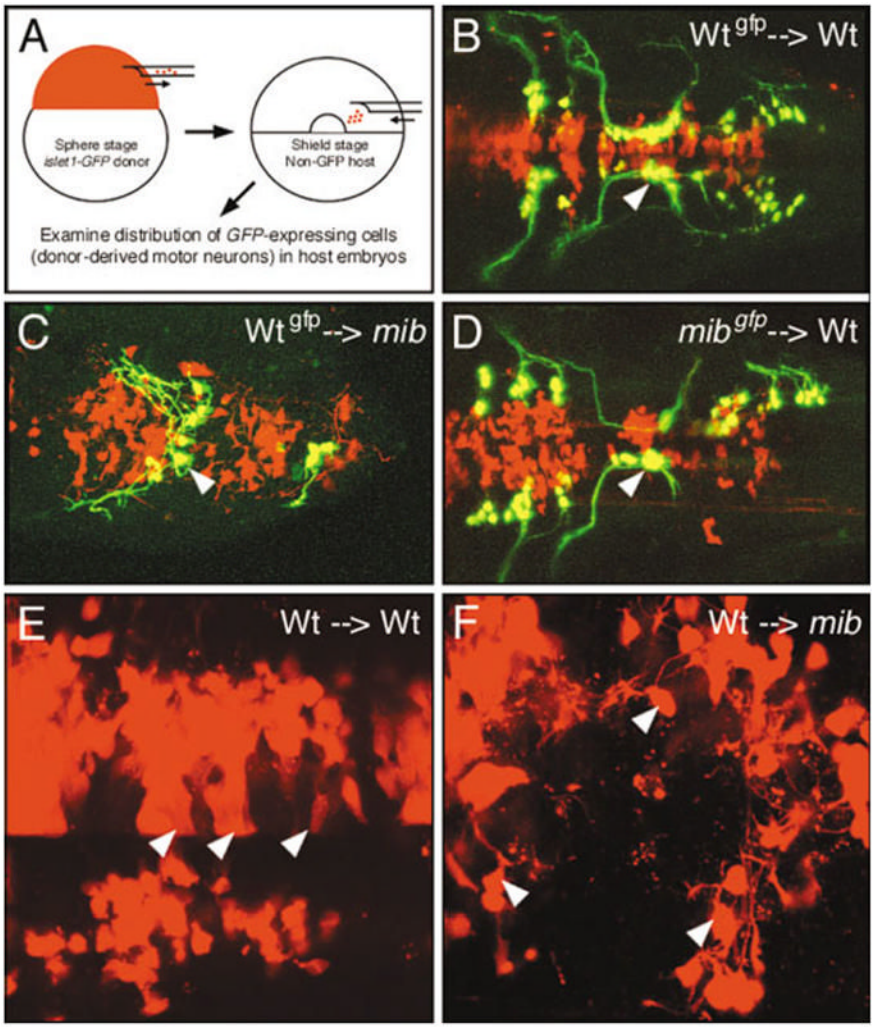

Fig. 6.

The *mind bomb* branchiomotor neuron (BMN) phenotype arises non–cell autonomously. B–F show dorsal views of the hindbrain with anterior to the left. In B–F, donor-derived cells are labeled red with rhodamine–dextran. In B–D, donor-derived BMNs are labeled yellow due to colocalization of *GFP* expression and rhodamine–dextran. **A:** The transplantation procedure. **B:** In a control experiment, wild-type (Wt) cells that differentiate into motor neurons (arrowhead) in a wild-type host are correctly organized into characteristic clusters. **C:** When donor-derived wild-type cells differentiate into motor neurons in a *mib* mutant host, the wild-type neurons (arrowhead) and their axons are loosely organized and straddle the midline, the characteristic mutant phenotype. **D:** When donor-derived *mib* mutant cells differentiate into motor neurons in a wild-type host, the mutant neurons (arrowhead) and their axons exhibit wild-type organization. **E:** In a wild-type host, many donor-derived cells exhibit a columnar morphology (arrowheads), suggestive of neuroepithelial cells. **F:** In a *mib* host, most donor-derived cells are round with short processes (arrowheads), suggestive of neurons.

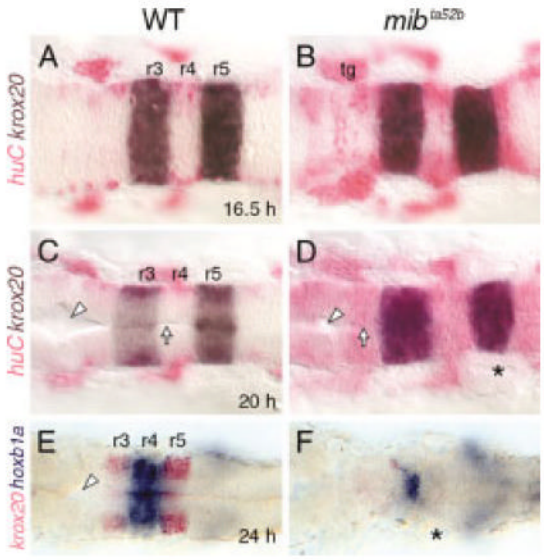

Fig. 7.

Rhombomere patterning is established but not maintained in *mind bomb* mutants. All panels show dorsal views with anterior to the left. Asterisks identify the otocyst. **A–D:** At 16.5 hours postfertilization (hpf; A,B) and 20 hpf (C,D), *krox20* is expressed normally in rhombomeres 3 and 5 (r3 and r5) in wild-type (WT) and mutant embryos, even though *huC*-expressing cells are greatly increased in the mutant hindbrains (B,D). By 20 hpf, the ventricular surface (arrow) and lumen (arrowhead) are well developed in the wild-type embryo (C) but are poorly developed in the mutant (D). **E,F:** In a *mib* mutant (F), *krox20* expression in r3 and r5 is absent, while *hoxb1a* expression in r4 is maintained but greatly reduced, compared with a wild-type sibling (E). In addition, the ventricle (arrowhead) seen in the wild-type embryo is missing in the mutant. tg, trigeminal ganglion.

TABLE 1

Branchiomotor Neurons Are Reduced in Number in *mind bomb* Mutants

Islet antibody-labeled cell type	WT (ta52b)[a]	*mib*^{ta52b}	Ratio (mutant/WT)
Total number of labeled cells in hindbrain[b]	205.9 ± 10.4 (11)	111.1 ± 15.5 (14)	0.54
Total number of labeled cells in r2 and r3 (nV neurons: Differentiate ≈18 hpf)	70.8 ± 7.8 (11)	51.5 ± 5.3 (14)	0.73
Total number of labeled cells in r4 to r7 (nVII neurons: Differentiate ≈15 hpf)	135.1 ± 8.6 (11)	59.1 ± 13.5 (14)	0.44
Number of labeled cells in ventral spinal cord[c] (Differentiate ≈ 24 hpf)	24.1 ± 1.6 (6)	12.9 ± 1.5 (6)	0.54
Number of Rohon–Beard cells[d] (Differentiate ≈10 hpf)	4.7 ± 0.4 (6)	9.8 ± 0.9 (6)	2.1

[a] Embryos were scored at 36 hours postfertilization (hpf). Numbers in parentheses represent number of embryos.

[b] The number corresponds to the total number of labeled cells (nV, nVII) in rhombomeres 2–7.

[c] Labeled cells (motor neurons and interneurons) were counted on one side in the ventral spinal cord in three contiguous segments at the level of the tip of the yolk tube. The number shown corresponds to the number of cells per hemisegment.

[d] Rohon–Beard cells, which are very darkly labeled cells in the dorsal-most neural tube, were counted on one side of the spinal cord in three contiguous segments at the level of the tip of the yolk tube. The number shown corresponds to the number of cells per hemisegment.

TABLE 2

Shh Overexpression Induces Ectopic Motor Neurons in *mind bomb* Mutants

	Injected RNA	No. of embryos[a]	Wild-type[b]	*mind bomb*[b]
Embryos with ectopic *GFP*- expressing cells in hindbrain[c]	None	197 (3)	0% (146)	0% (51)
	shh	231 (3)	94% (159)	100% (72)
Number of islet antibody-labeled cells in hindbrain[d]	None	5 (1)	188 ± 16.6	104.7 ± 9
	shh	5 (1)	277.4 ± 11.4	148.8 ± 23
	Ratio (*shh* / control)		1.48	1.42

[a] Numbers in parentheses represent number of experiments.

[b] Numbers in parentheses represent number of embryos. Embryos were scored as mutant if the branchiomotor neurons exhibited fusion across the midline (Fig. 3B and D). The mutant embryo in Fig. 3D exhibited an unusually large increase in motor neuron number.

[c] Embryos (36 hours postfertilization) were considered to have ectopic expression if the number of *GFP*-expressing branchiomotor neurons were increased relative to uninjected controls. The ectopic neurons were especially evident in rhombomeres 2 and 4 (Compare Fig. 3A and C), where ectopic neurons were located dorsally along the lateral margin of the neural tube, and in the caudal hindbrain.

[d] The number corresponds to the total number of labeled cells (nV, nVII) in rhombomeres 2–7.

TABLE 3

Defects in Ventral Neural Tube Gene Expression in the *mind bomb* Mutant Hindbrain[a]

		Defect in Expression Pattern		
Gene	**Genotype**	**No Defects**	**Gap in r2/r3**	**Gap in r4**
shh (25 hpf)	Wild-type (20)	20/20	0/20	0/20
	Mutant (14)	6/14	2/14	6/14
nk2.2 (24 hpf)	Wild-type (20)	20/20	0/20	0/20
	Mutant (24)	6/24	1/24	17/24
net1b (30 hpf)	Wild-type (20)	20/20	0/20	0/20
	Mutant (52)	16/52	0/52	36/52

[a]Number of embryos are shown in parentheses. Gaps in rhombomeres 2, 3, and 4 (r2, r3, r4) were scored, while gaps in the caudal hindbrain, which were infrequent, and other defects in expression pattern were excluded from analysis. The position of the gap in expression was determined relative to the outlines of the otic vesicle, which spans rhombomeres 4–6 at the developmental stages examined. hpf, hours postfertilization.